THE JOURNAL OF PHYSICAL CHEMISTRY C

Article

pubs.acs.org/JPCC

Enhanced Photovoltaic Performance of Diketopyrrolopyrrole (DPP)-Based Polymers with Extended π Conjugation

Shaoqing Zhang,[†,‡] Long Ye,[‡] Qi Wang,[†,‡] Zhaojun Li,[†,‡] Xia Guo,[‡] Lijun Huo,[‡] Huili Fan,*[,†] and Jianhui Hou*[,†,‡]

[†]University of Science and Technology Beijing, School of Chemistry and Biology Engineering, Beijing 100083, China

[‡]State Key Laboratory of Polymer Physics and Chemistry, Beijing National Laboratory for Molecular Sciences Institute of Chemistry, Chinese Academy of Sciences, Beijing 100190, China

Supporting Information

ABSTRACT: To extend the π conjugation along backbone units is an effective way to tune the optoelectronic properties of conjugated polymers. In this work, to investigate the influence of the extended conjugation on photovoltaic properties of the polymer, we employed a two-step molecular optimization process, and a series of diketopyrrolopyrrole (DPP)-based conjugated polymers, PBDPP-1, PBDPP-2, and PBDPP-3, was prepared and applied in polymer solar cells. After this two-step optimization of molecular structure, the compatibility between the polymer and $PC_{71}BM$ becomes much better; as a result, bicontinuous phase separation with appropriate domain size can be formed in the blend of PBDPP-3/$PC_{71}BM$. Therefore, the PBDPP-3/$PC_{71}BM$-based device shows a short circuit current density (J_{sc}) of 16.25 mA/cm^2, which is more than two times of that of the PBDPP-1/$PC_{71}BM$-based device. In addition, the blend films processed by DIO/CB showed smoother surfaces as well as smaller domain size compared with the blend films processed by pure CB. The results in this work indicate that when conjugation of the DPP-polymer's backbone is extended in two dimensions the morphology of the active layers in photovoltaic device can be optimized effectively, and hence the overall efficiency can be improved from 2.83 to 6.18%.

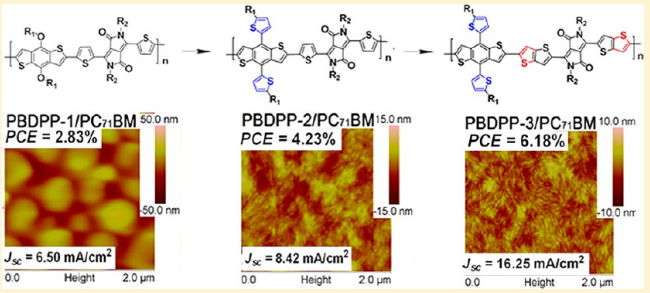

INTRODUCTION

Many kinds of conjugated polymers have been developed for the application in polymer solar cells (PSCs). The optimization of molecular structure of photovoltaic polymers is of great importance to realize high photovoltaic performance. To realize high efficiency, conjugated polymers with ideal properties, like broad and strong absorption, appropriate molecular energy level, high mobility, and so on are requisite. Therefore, different strategies have been developed and applied in molecular structure design of photovoltaic polymers. For instance, building conjugated backbones with donor−acceptor (D-A) alternative structure and introducing conjugated building blocks with strong quinoid properties have been used as two effective approaches to realize low band gap (LBG) in conjugated polymers. According to these two approaches, many backbone structures of LBG polymers, such as PSBTBT,[1] PCPDTBT,[2] PCDTBT,[3] PFDTBT,[4] PBDTTT,[5] PBDTDTBT,[6] PBDTTPD,[7] and so on, have been successfully designed, synthesized, and applied in PSCs. In the past several years, these backbone structures are contributed to many important progresses in the PSC field. Fine-tuning of molecular structure also plays an important role in photovoltaic polymer design. For instance, the highest occupied molecular orbit (HOMO) and the lowest unoccupied molecular orbit (LUMO) levels of photovoltaic polymers can be modulated by tuning the electron-withdrawing/donating effects of their substituents;[5a,8] morphological properties, such as crystallinity, molecular orientation, and other properties of conjugated polymers can also be controlled or modulated by changing their functional groups. Consequently, the three key parameters of PSC devices, that is, short circuit current density (J_{sc}), open circuit voltage (V_{oc}), and fill factor (FF), can be improved separately or simultaneously, and hence high power conversion efficiencies (PCEs) can be realized.[9]

To extend the π conjugation along backbone units is an effective way to tune the optoelectronic properties of conjugated polymers. First, optical absorption property of conjugated polymers is closely related to π-electron delocalization ability. The strategy of improving π-electron delocalization is helpful to realize LBG. For example, to improve planarity of conjugated backbone by reducing steric hindrance between adjacent backbone units has been broadly used to enhance absorption of conjugated polymers;[10] the introduction of 2D conjugated structure has been proven to be an effective way to get polythiophenes (PTs) with panchromatic absorption band.[11,12] Second, organic materials, including small molecules

Received: December 18, 2012
Revised: April 23, 2013

   dx.doi.org/10.1021/jp312450p | J. Phys. Chem. C XXXX, XXX, XXX−XXX

Scheme 1. Molecular Structures and Synthesis of Three BDT- and DPP-Based Polymers

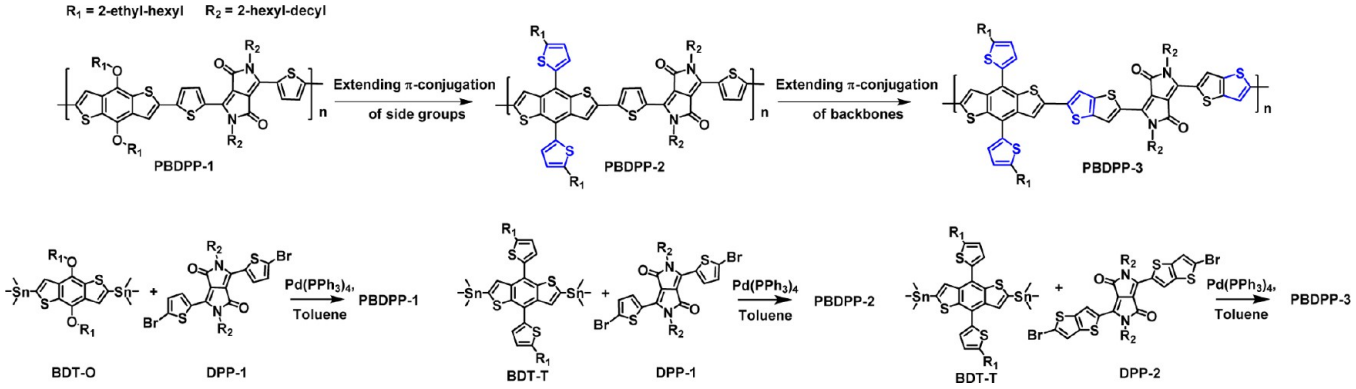

and polymers, with well-delocalized π electrons exhibit superiority in charge transport. For instance, the π electrons of pentacene and its derivatives show excellent delocalization ability and low binding energy, and hence mobilities of ~3 $cm^2 V^{-1} s^{-1}$ have been recorded,[13] which are among the highest values in the field of organic electronics.

Recently, our group carried out systematic studies to investigate the influence of photovoltaic properties of benzodithiophene (BDT)-based polymers by extending π conjugation of their backbones. We introduced 2D conjugated structure into BDT-polymers by replacement of alkoxy with alkylthienyl. For example, compared with PBDTTT-C, the PSC device based on PBDTTT-C-T showed an improved PCE of 7.6% by using the 2D conjugated BDT unit.[14] Furthermore, the advantages of the 2D conjugated BDT have been verified in different polymer systems.[10,15] These works indicated that to extend π-conjugation of conjugated polymers is helpful to improve their photovoltaic properties, and the study on the correlation among π conjugation of backbone units, morphological and optical properties, as well as photovoltaic behaviors is still an important topic in molecular structure design of conjugated polymers for the applications in PSCs.

The polymers based on 2,5-dialkyl-3,6-dithiophene-2-yl-dropyrrolo[3,4-*c*]pyrrole-1,4-dione) (DPP) play important roles in PSCs[16] and organic field effect transistors (OFETs).[17] For instance, PDPP3T[18] can be used as an electron donor material in PSCs and showed a PCE of 4.7%, and after optimizing the morphology of the PDPP3T/PCBM blend film by using ternary solvents, a PCE of 6.71% can be achieved.[19] Because DPP-polymers show broad and strong absorption bands covering visible and near-infrared light region, they are good candidates as red absorbers for the applications in PSCs with tandem structure; for instance, a PCE of 8.62% has been recently reported by using a DPP-based polymer as a red absorber material.[20] Some DPP-polymers also show excellent charge-transport properties; mobilities over 1 $cm^2 V^{-1} s^{-1}$ for hole[21] and 0.1 $cm^2 V^{-1} s^{-1}$ for electron[22] have been realized in the OFETs. Considering that DPP-polymers are potential organic semiconducting materials, to reveal the correlation between the extended π-conjugation of backbone units and photovoltaic properties of DPP-polymers will be an interesting and also important topic in the field.

RESULTS AND DISCUSSION

Molecular Design and Synthesis. Herein, starting from PBDPP-1, as shown in Scheme 1, two DPP-polymers named as PBDPP-2 and PBDPP-3, were designed and synthesized by extending the π-conjugation perpendicular to and along the backbone; that is, from PBDPP-1 to PBDPP-2, the conjugation perpendicular to the backbone of the polymer was extended by replacing alkoxy with alkylthienyl groups; then, from PBDPP-2 to PBDPP-3, the conjugation along the backbone was extended by replacing thiophene with thieno[3,2-*b*]thiophene units. The synthesis methods of these three polymers are provided in Scheme 1. The polymers were prepared through a Stille coupling reaction between the bis(trimethyltin)-BDT monomers (BDT-T and BDT-O) and the bromides (DPP-1 and DPP-2). The number-average molecular weights (M_n) of PBDPP-1, PBDPP-2, and PBDPP-3 are 40K (PDI = 2.5), 32K (PDI = 1.9), and 21K (PDI = 2.3), respectively. These three polymers can be readily dissolved in chloroform ($CHCl_3$), chlorobenzene (CB), and *o*-dichlorobenzene (*o*-DCB).

Thermogravimetric analysis (TGA) measurements were employed to evaluate the thermal stability of the polymers. The TGA plots of these three polymers are shown in Figure 1,

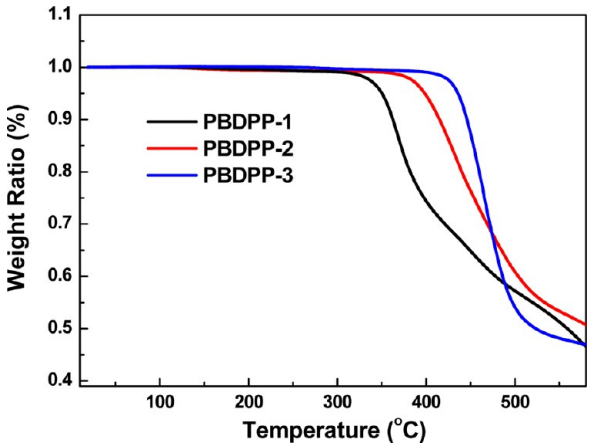

Figure 1. TGA plots of these three polymers with a heating rate of 10 °C/min under the inert atmosphere.

and their decomposition temperatures (T_d) are collected in Table 1. The comparisons among these T_d values reveal that after extending the conjugation, thermal stability of the DPP-polymer can be improved obviously. As a result, T_d of PBDPP-3 reaches 422 °C, which is much higher compared with that of PBDPP-1.

Absorption Spectra and Electrochemical Properties. The absorption spectra of these three polymers in dilute chlorobenzence solution and solid films are shown in Figure

dx.doi.org/10.1021/jp312450p | J. Phys. Chem. C XXXX, XXX, XXX–XXX

Table 1. Optical and Electrochemical Properties of Four BDT- and DPP-Based Polymers

	T_d (°C)	λ_{max} (nm) soln.	λ_{max} (nm) film	E_g^{opt} (eV)	HOMO (eV)	LUMO (eV)	μ_{hole} ($cm^2/(V\ s)$)
PBDPP-1	330	752	752	1.45	−5.29	−3.84	4.48×10^{-2}
PBDPP-2	390	766	775	1.45	−5.29	−3.84	2.35×10^{-2}
PBDPP-3	422	768	772	1.43	−5.05	−3.62	1.16×10^{-1}

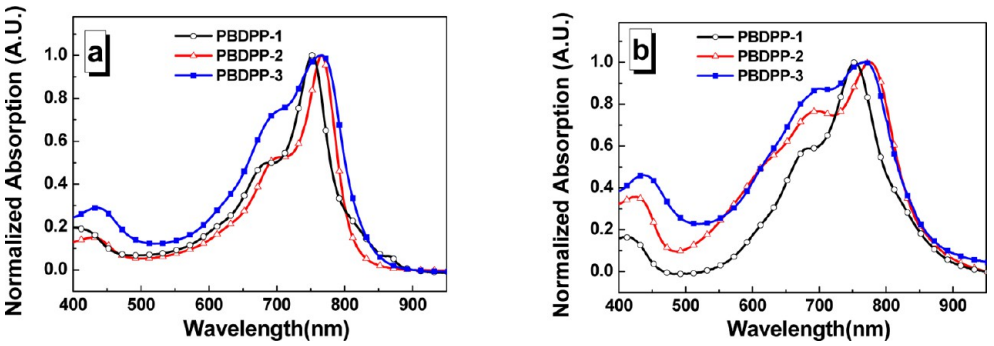

Figure 2. Absorption spectra of three BDT and DPP based polymers (a) in chloroform solution and (b) of solid films.

2a,b, respectively, and the detailed absorption data are collected in Table 1. These three polymers show similar absorption onsets at ca. 880 nm, corresponding to a band gap (E_g) of 1.4 eV. The absorption peaks of PBDPP-1 in solution and solid film are at ∼752 nm, while the absorption peaks of PBDPP-2 and PBDPP-3 are at ∼770 nm. From PBDPP-1 to PBDPP-2 and then to PBDPP-3, the absorption in both long and short wavelength directions is improved effectively. As a result, the final polymer, PBDPP-3, shows the broadest absorption band in comparison with the other two polymers. Therefore, it can be concluded that the extended π-conjugation is helpful to improve photoabsorption properties of the DPP-polymers.

Electrochemical cyclic voltammetry (CV) is performed to evaluate molecular energy levels of conjugated polymers.[23] Figure 3 shows the CV plots of these three DPP-polymers' films on glassy carbon electrode. The onset points of p-doping process of PBDPP-1, PBDPP-2, and PBDPP-3 are at 0.49, 0.49, and 0.25 V, corresponding to HOMO levels of −5.29, −5.29, and −5.05 eV, respectively. Because it is very hard to get a sharp *n*-doping signal for these three polymers, the LUMO levels of the polymers were estimated by "LUMO = HOMO − E_g^{opt}". According to the CV results, it is clear that after extending π conjugation of the backbone perpendicularly by replacing alkoxy with alkylthienyl, the HOMO level of the DPP-polymer was little changed, whereas when π conjugation along the backbone was extended by replacing thiophene with thieno[3,2-b]thiophene, the HOMO level of the DPP-polymer was elevated obviously. Because V_{oc} of bulk heterojunction PSCs is directly proportional to the offset between HOMO level of the donor and LUMO level of the acceptor,[24] V_{oc} of PBDPP-3-based PSC might be lower than those of PBDPP-1- and PBDPP-2-based devices.

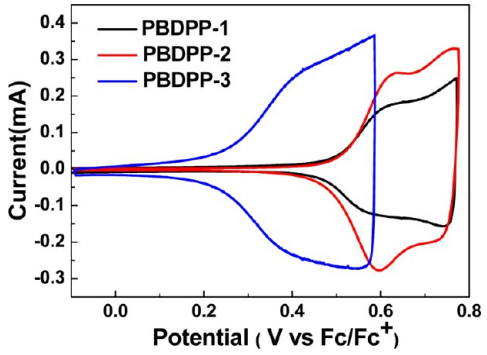

Figure 3. Cyclic voltammograms of PBDPP-1, PBDPP-2, and PBDPP-3 films on the glassy carbon electrode in 0.1 mol/L Bu_4NPF_6 in acetonitrile solution at a scan rate of 50 mV/s.

X-ray Diffraction Analysis. X-ray diffraction (XRD) measurement has been used to investigate the formation of ordered structures within thin films. Figure 4 shows the XRD patterns of the films of three polymers casted from CB. The films of PBDPP-1 show very weak reflections at 2θ = 5.13° (corresponding to a laminar *d* spacing of 17.2 Å) and 2θ = 24.2° (corresponding to a $\pi-\pi$ stack *d* spacing of 3.67 Å), while no reflection peak can be observed in the film of PBDPP-2. However, two clear reflection peaks, 2θ = 4.41° (corresponding to a laminar *d* spacing of 20.0 Å) and 2θ = 24.7°(corresponding to a $\pi-\pi$ stack *d* spacing of 3.60 Å), can be distinguished in the XRD plot of the film of PBDPP-3. The comparison among the XRD patterns of the three films clearly indicates that more ordered structure can be formed in the film of PBDPP-3, implying that the interchain packing as well as the $\pi-\pi$ stacking of the polymer can be enhanced by extending the conjugation along the backbones, that is, by replacing thiophene units with

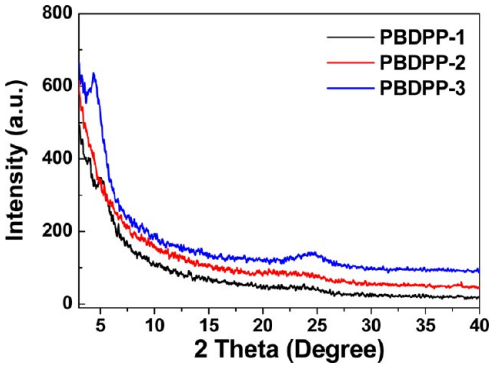

Figure 4. X-ray diffraction patterns of three polymers films casted from CB onto Si substrates.

dx.doi.org/10.1021/jp312450p | J. Phys. Chem. C XXXX, XXX, XXX−XXX

thieno[3,2-b]thiophene units, while the introduction of alkylthienyl groups in BDT units has little influence on the crystallinity of the polymer. Furthermore, we measured the hole mobilities of these three polymers by using the space-charge-limited current (SCLC) method.[25] As listed in Table 1, the hole mobilities of the thin films of PBDPP-1, PBDPP-2, and PBDPP-3 are 4.48×10^{-2}, 2.35×10^{-2}, and 1.16×10^{-1} $cm^2/(V\ s)$, respectively, implying that ordered laminar packing and intermolecular $\pi-\pi$ stacking may benefit from hole transport of the polymer.

Photovoltaic Properties. To investigate the photovoltaic properties of these three polymers, we fabricated the PSC devices with a structure of ITO/PEDOT-PSS/polymer:$PC_{71}BM$/Ca/Al. CB was used to prepare the solutions for spin-coating of the active layers, and the concentration of the solutions used in this work was 6 mg/mL (polymer/CB). Thickness of the active layers of the devices was controlled by changing spin speed. Initially, varied D/A (polymer/$PC_{71}BM$, wt/wt) ratios, 1:1, 1:2, and 1:3, were scanned. We found that the optimal D/A ratio for all of these three polymers is 1:2, which is consistent with the reported works.[16b] Because 1,8-diiodooctane (DIO) has been widely and successfully used as an additive during spin-coating process for fabrication of PSC devices,[2b] it was adopted to further improve photovoltaic performance in this work. Herein, varied amounts of DIO, that is, 0.5, 1, 2, and 3% (v/v, DIO/CB), were scanned to optimize photovoltaic properties of the devices. The $J-V$ curves of the devices with varied amounts of DIO are provided in Figures S1–S3 as Supporting Information (SI), and the photovoltaic parameters are listed in Tables S1–S3 in the Supporting Information; we found that the devices of PBDPP-1 and PBDPP-2 showed optimal photovoltaic performance when 3% DIO was used, while for the devices of PBDPP-3 the optimum ratio of DIO is 0.5%.

Figure 5 shows the $J-V$ curves of the devices of these three polymers without and with the addition of an optimum amount

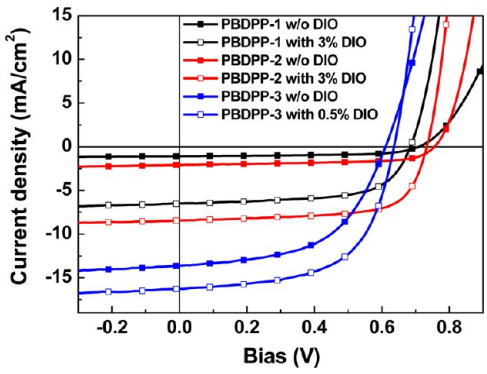

Figure 5. $J-V$ curves of the devices of PBDPP-1, PBDPP-2, and PBDPP-3 with a D/A ratio of 1:2 (polymer/$PC_{71}BM$, wt/wt), processed without and with the use of optimum amount of DIO.

of DIO, and the key photovoltaic parameters are listed in Table 2. As shown, V_{oc} of the devices of PBDPP-1 and PBDPP-2 is between 0.70 and 0.74 V, which is 0.1 V higher compared with that of the devices of PBDPP-3. The lower V_{oc} of the devices of PBDPP-3 should be ascribed to the higher HOMO level of the polymer. Without the use of DIO, the devices of PBDPP-1 and PBDPP-2 show very low J_{sc}, that is, 1.16 and 2.07 mA/cm^2, respectively, while the device of PBDPP-3 prepared without the use of DIO shows a J_{sc} of 13.60 mA/cm^2; consequently, PCE of the device of PBDPP-3 is 4.52%, which is much higher than the devices of the other two polymers. With the use of optimum amount (3%) of DIO, J_{sc} of the devices of PBDPP-1 and PBDPP-2 was improved tremendously, reaching 6.50 and 8.42 mA/cm^2, respectively, and as a result, PCEs of these two kinds of devices got to 2.83 and 4.23%, respectively; similarly, with the use of 0.5% DIO, J_{sc} of the device of PBDPP-3 increased to 16.25 mA/cm^2 and PCE of the device reached 6.18%. In addition, all of the devices of three polymers processed with the use of DIO show higher FF compared with the devices without the use of DIO.

Absorption spectra of the active layers and external quantum efficiency (EQE) curves of the devices based on these three polymers prepared through the optimal fabrication processes are shown in Figure 6a,b. It is clear that benefiting from the low optical band gaps of the polymers and the complementary photoabsorption from $PC_{71}BM$, these three kinds of devices show a very broad response range, covering from 350 to 880 nm. According to the absorption spectra of the films, as shown in Figures 2b and 6a, absorption of the active layers in short wavelength region, from 400 to 600 nm, is mainly contributed by $PC_{71}BM$; absorption of the active layers in long wavelength region, from 600 to 900 nm, is attributed to the polymers. Although these three kinds of devices have similar photoabsorption properties, quantum efficiency of the device of PBDPP-3 is much higher than the other two kinds of devices. Interestingly, although these three devices show similar absorption spectra, the shapes of their EQE curves are much different. For the devices of PBDPP-1 and PBDPP-2, EQE values at long wavelength direction are obviously lower than that at short wavelength region, implying that in these two kinds of devices the photons absorbed by $PC_{71}BM$ can be converted to the photocurrent more efficiently compared with those absorbed by polymer, whereas for the device of PBDPP-3, the photons absorbed by $PC_{71}BM$ as well as by polymer contribute evenly to the photocurrent of the device.

Morphology Study. The morphological properties of the polymer/$PC_{71}BM$ blend films were tested by using atomic force microscopy (AFM). To investigate the influence of the use of DIO during spin-coating processes on morphology of the blend films, we show AFM images of the blend films of PBDPP-1/$PC_{71}BM$, PBDPP-2/$PC_{71}BM$, and PBDPP-3/$PC_{71}BM$ processed without and with optimum amount of DIO in Figure 7a–l. For the blend film of PBDPP-1/$PC_{71}BM$ processed without DIO, big size aggregations, that is, over a few hundreds of nanometers, can be observed in both the height and the phase images (see Figure 7a,b), and also the mean square surface roughness (R_q) of the film is very high (R_q = 35.0 nm); after the use of DIO (see Figure 7c,d), the size of the aggregation was little influenced, but the film surface became smoother (R_q = 8.66 nm); therefore, the improved efficiency of the PBDPP-1/$PC_{71}BM$ device by the use of DIO should be attributed to the improved surface quality. For the blend film of PBDPP-2/$PC_{71}BM$ processed without DIO, big size aggregations, as observed in PBDPP-1/$PC_{71}BM$, can be found in both the height and the phase images (see Figure 7e,f), whereas after the use of DIO, the aggregations became much smaller and the R_q value of the film was reduced from 17.4 to 3.05 nm (see Figure 7g,h), and hence the improved efficiency of the PBDPP-2/$PC_{71}BM$ device by the use of DIO should be ascribed to both the improved surface quality and the formation of bicontinuous phase separation with smaller size aggregations. For the blend of film of PBDPP-3/$PC_{71}BM$ processed without DIO, the sizes

dx.doi.org/10.1021/jp312450p | J. Phys. Chem. C XXXX, XXX, XXX–XXX

Table 2. Photovoltaic Parameters of the Devices of PBDPP-1, PBDPP-2, and PBDPP-3 with a D/A ratio of 1:2 (polymer/$PC_{71}BM$, wt/wt) processed without and with the Use of Optimum Amount of DIO

	DIO additive	V_{oc} (V)	J_{sc} (mA/cm^2)	FF	PCE (%)	thickness (nm)
PBDPP-1	w/o	0.71	1.16	0.61	0.50	110
	3%	0.69	6.50	0.63	2.83	103
PBDPP-2	w/o	0.75	2.07	0.63	0.99	117
	3%	0.73	8.42	0.68	4.23	96
PBDPP-3	w/o	0.61	13.60	0.54	4.52	106
	0.5%	0.63	16.25	0.60	6.18	110

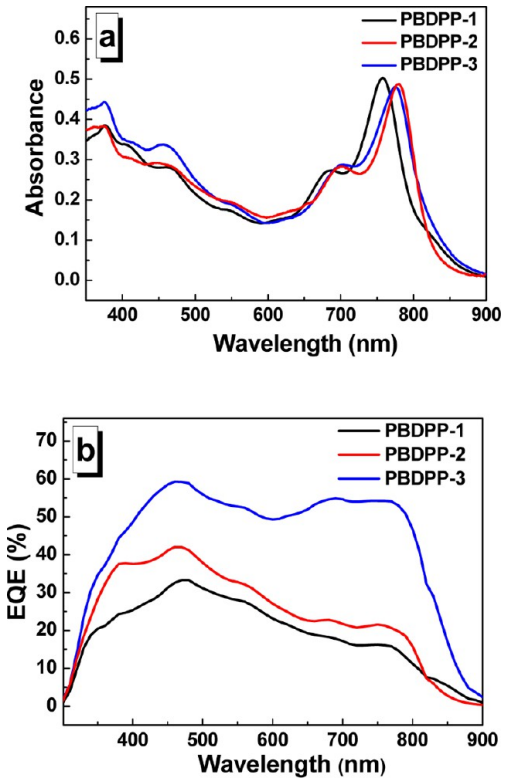

Figure 6. Absorption spectra (a) of the active layers and EQE curves (b) of the PSC devices of PBDPP-1, PBDPP-2, and PBDPP-3 fabricated by the optimal conditions.

of both the aggregations and the surface roughness are obviously smaller (see Figure 7i,j, R_q = 6.25 nm) compared with those of the films of PBDPP-1/$PC_{71}BM$ and PBDPP-2/$PC_{71}BM$; after the use of 0.5% DIO, the regular fibrillar shape domains (3−5 nm in width and tens of nanometer in length) can be observed in both the height and the phase images (see Figure 7k,l), and also the film showed good surface quality (R_q = 1.81 nm). As known, the optimal domain size in the D/A blend of heterojunction solar cells is ∼10−20 nm because the exciton diffusion length is 10−20 nm.[26] Therefore, morphology of the PBDPP-3/$PC_{71}BM$ blend is more favorable than that of the other two kinds of blend films, which explains the better EQE of the PBDPP-3/$PC_{71}BM$ device. In our previous work, by introducing extended π conjugation of a LBG polymer, crystallinity of the polymer can be improved effectively, while the domain size in the D/A blend has not been affected.[27] The morphology study in this work indicates that the extended π conjugation of DPP-based polymer is also helpful to improve the compatibility between the polymer and PCBM.

Furthermore, transmission electron microscope (TEM) was used to confirm the findings in AFM measurements. TEM images of the blend films of PBDPP-1/$PC_{71}BM$, PBDPP-2/$PC_{71}BM$, and PBDPP-3/$PC_{71}BM$ processed with optimum amount of DIO are shown in Figure 8a−c. As shown in Figure 8a, ball-like dark domains with diameters between 100 and 400 nm can be observed, which should be due to the aggregation of $PC_{71}BM$; in Figure 8b, the aggregations of $PC_{71}BM$ are much smaller, but the blend film is still not uniform; that is, the light domains, corresponding to the aggregations of the polymer, can be clearly observed. In Figure 8c, the whole image looks very uniform, meaning that bicontinuous phase separation with small polymer domains and $PC_{71}BM$ domains is formed. Overall, the observations of TEM measurements are coincident with the findings obtained from AFM measurements very well.

CONCLUSIONS

A two-step molecular optimization process was employed, and a series of DPP-based conjugated polymers, PBDPP-1, PBDPP-2, and PBDPP-3, were prepared and applied in PSC devices to investigate the influence of the extended conjugation on photovoltaic properties of the polymer. From PBDPP-1 to PBDPP-2 and then to PBDPP-3, the molecular structures of the polymers were optimized by improving the conjugation perpendicular to and along the backbones successively. We found that after this two-step optimization of molecular structure, compared with the starting polymer, the absorption band of the final polymer is broadened obviously and the laminar packing as well the intermolecular $\pi-\pi$ stacking can be improved. We also observed that after extending the conjugation along the backbone, the HOMO level of the DPP-polymer is elevated so that the device of PBDPP-3 shows lower V_{oc} than the devices of the other two polymers.

As observed in AFM and TEM measurements, the compatibility between PBDPP-1 and $PC_{71}BM$ is quite low so that huge aggregations can be formed in the PBDPP-1/$PC_{71}BM$ blend, which is detrimental to realizing efficient photovoltaic performance; after this two-step optimization of molecular structure, the compatibility between the polymer and $PC_{71}BM$ becomes much better, and as a result, bicontinuous phase separation with appropriate domain size can be formed in the blend of PBDPP-3/$PC_{71}BM$. Therefore, the PBDPP-3/$PC_{71}BM$-based device shows a J_{sc} of 16.25 mA/cm^2, which is more than two times that of the PBDPP-1/PCBM-based device. In addition, the influence of the use of DIO on morphologies of the polymer/$PC_{71}BM$ blends was also clearly revealed; that is, the blend films processed by DIO/CB showed smoother surfaces as well as smaller domain size compared with the blend films processed by pure CB. Overall, this work demonstrated a full picture of a two-step optimization of DPP polymers by extending the conjugation perpendicular to and along the backbone successively and thus provides a guideline for molecular design of photovoltaic polymers.

dx.doi.org/10.1021/jp312450p | J. Phys. Chem. C XXXX, XXX, XXX−XXX

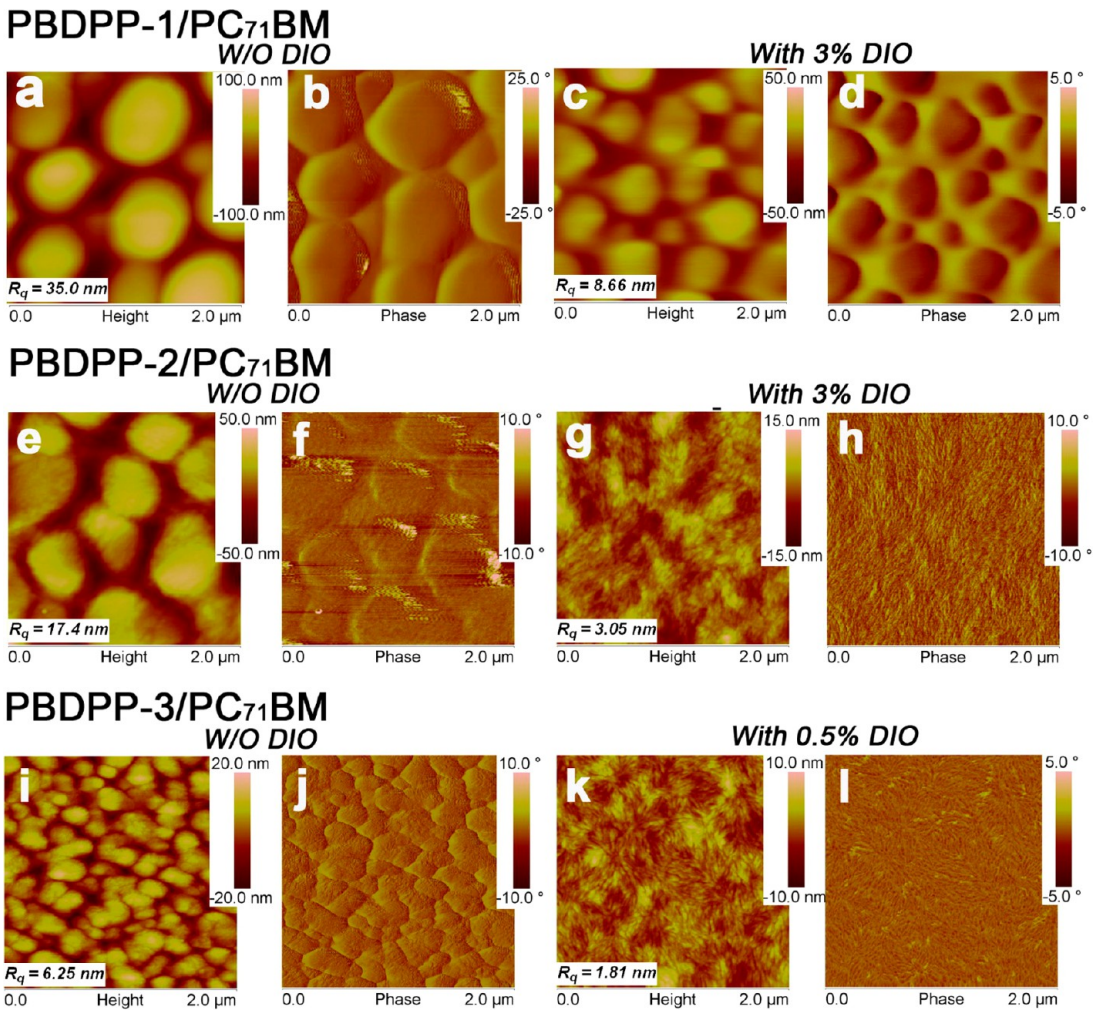

Figure 7. AFM images of the blend films of PBDPP-1/$PC_{71}BM$, PBDPP-2/$PC_{71}BM$, and PBDPP-3/$PC_{71}BM$ processed without and with optimum amount of DIO.

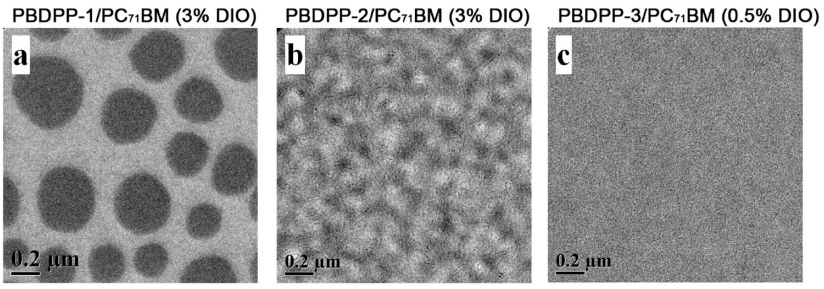

Figure 8. TEM images of the blend films of (a) PBDPP-1/$PC_{71}BM$, (b) PBDPP-2/$PC_{71}BM$, and (c) PBDPP-3/$PC_{71}BM$ processed with optimum amount of DIO.

EXPERIMENTAL SECTION

Materials. The monomers, BDT-O, BDT-T, DPP-1, and DPP-2, are obtained from Solarmer Materials. $Pd(PPh_3)_4$ was purchased from Frontier Chemical. The other materials were of common commercial level and used as received.

Instruments and Measurements. UV−visible absorption spectroscopy measurements were carried out using a Hitachi U-3100 UV−vis spectrophotometer. Atom force microscopy (AFM) was performed on a Nanoscope III A (Vecco) AFM by the tapping mode. Molecular weight and polydispersity (PDI) of the polymers were estimated by gel permeation chromatography (GPC) method using monodispersed polystyrene as standard and chloroform as eluent (at 45 °C). The CV measurements were conducted on a CHI650D electrochemical workstation with Pt disk, Pt plate, and Ag/Ag^+ electrode as working electrode, counter electrode, and reference electrode, respectively, in a 0.1 M tetrabutylammonium hexafluorophosphate (Bu_4NPF_6) acetonitrile solution. The potential of Ag/Ag^+ reference electrode was internally calibrated by using the ferrocene/ferrocenium redox couple (Fc/Fc^+). The thicknesses of the PEDOT:PSS and active layer were determined by an Ambios Tech. XP-2 profilometer. The current density−voltage (J−V) characteristics were recorded

dx.doi.org/10.1021/jp312450p | J. Phys. Chem. C XXXX, XXX, XXX−XXX

with a Agilent B2912A precision source/measure unit. The PCEs of the resulting PSCs were measured under AM 1.5G (air mass 1.5 global) spectrum from a solar simulator (100 mW/cm^2) using an XES-70S1 (SAN-EI Electric) solar simulator (AAA grade, 70 mm × 70 mm photobeam size). We purchased 2 × 2 cm monocrystalline silicon reference cell (SRC-1000-TC-QZ) from VLSI Standards. The EQE was measured by solar cell spectral response measurement system QE-R3011 (Enli Technology). The light intensity at each wavelength was calibrated with a standard single-crystal Si photovoltaic cell.

Fabrication of Polymer Solar Cells. PSC devices with the structure of ITO/PEDOT-PSS/Polymers:$PC_{71}BM$/Ca(10 nm)/Al(80 nm) were fabricated under conditions as follows: patterned indium tin oxide (ITO)-coated glass with a sheet resistance of 10−15 ohm/square was cleaned by a surfactant scrub and then washed by deionized water, acetone, and isopropanol, successively. After UV-ozone cleaning for 10 min, a 30−40 nm thick poly(3,4-ethylenedioxythiophene):poly-(styrenesulfonate) (PEDOT:PSS) (Bayer Baytron 4083) anode buffer layer was spin-cast onto the ITO substrate and then dried in an oven at 150 °C for 15 min. The active layer, with a thickness in the range of 80−110 nm, was then deposited on top of the PEDOT:PSS layer by spin-coating from a solution of certain concentration (6 mg/mL). Finally, 10 nm Ca and 80 nm Al layer were successively deposited under high vacuum (ca. 3 × 10^{-4} Pa) onto the active layer. The overlapping area between the cathode and anode defined a pixel size of 4 mm^2. Except for the deposition of the PEDOT:PSS layers, all fabrication processes were carried out inside a nitrogen drybox containing <10 ppm oxygen and moisture.

Synthesis. *Polymerization of PBDPP-1, PBDPP-2, and PBDPP-3.* The dibromide monomer (DPP-1 or DPP-2) (0.5 mmol) and the bis-trimethyltin-monomer (BDT-O or BDT-T) (0.5 mmol) were dissolved in 15 mL of toluene in a flask protected by argon. After flushing by argon for 5 min, 20 mg of $Pd(PPh_3)_4$ was added to the flask. The reactant was purged by argon for another 20 min and then heated to 110 °C. The reactant was stirred at 110 °C for 18 h under the inert atmosphere and then cooled to room temperature. The polymer was precipitated from 100 mL of methanol as small fibrils. The precipitated polymer was collected and exacted by methanol, hexane, and chloroform successively. The polymer was obtained as dark green solid with a yield of ∼60%. PBDPP-1: Calculated for $C_{72}H_{106}N_2O_4S_4$: C, 72.55%; H, 8.96%; N, 2.35%; found: C, 72.77%; H, 9.24%; N, 2.45%. PBDPP-2: Calculated for $C_{80}H_{112}N_2O_2S_6$: C, 72.45%; H, 8.51%; N, 2.11%; found: C, 72.38%; H, 8.38%; N, 2.30%. PBDPP-3: Calculated for $C_{84}H_{110}N_2O_2S_8$: C, 70.24%; H, 7.72%; N, 1.95%; found: C, 69.91%; H, 7.74%; N, 2.07%.

■ ASSOCIATED CONTENT

Ⓢ Supporting Information

Photovoltaic data of PSC devices of these three polymers are provided. This material is available free of charge via the Internet at http://pubs.acs.org.

■ AUTHOR INFORMATION

Corresponding Author

*E-mail: hjhzlz@iccas.ac.cn; fanhl@sas.ustb.edu.cn. Tel: +86-10-82615900.

Notes

The authors declare no competing financial interest.

■ ACKNOWLEDGMENTS

We acknowledge the financial support from National High Technology Research and Development Program 863 (2011AA050523), Chinese Academy of Sciences (KJ2D-EW-J01), Ministry of Science and Technology of China, NSFC (nos. 51173189, 21104088),and International S&T Cooperation Program of China (2011DFG63460).

■ REFERENCES

(1) (a) Hou, J.; Chen, H. Y.; Zhang, S.; Li, G.; Yang, Y. Synthesis, Characterization, and Photovoltaic Properties of a Low Band Gap Polymer Based on Silole-Containing Polythiophenes and 2,1,3-Benzothiadiazole. *J. Am. Chem. Soc.* **2008**, *130*, 16144−16145. (b) Chen, H. Y.; Hou, J.; Hayden, A. E.; Yang, H.; Houk, K. N.; Yang, Y. Silicon Atom Substitution Enhances Interchain Packing in a Thiophene-Based Polymer System. *Adv. Mater.* **2010**, *22*, 371−375.

(2) (a) Zhu, Z.; Waller, D.; Gaudiana, R.; Morana, M.; Mu1hlbacher, D.; Scharber, M.; Brabec, C. Panchromatic Conjugated Polymers Containing Alternating Donor/Acceptor Units for Photovoltaic Applications. *Macromolecules* **2007**, *40*, 1981−1986. (b) Peet, J.; Kim, J. Y.; Coates, N. E.; Ma, W. L.; Moses, D.; Heeger, A. J.; Bazan, G. C. Efficiency Enhancement in Low-Bandgap Polymer Solar Cells by Processing with Alkane Dithiols. *Nat. Mater.* **2007**, *6*, 497−500.

(3) Blouin, N.; Michaud, A.; Gendron, D.; Wakim, S.; Blair, E.; Neagu-Plesu, R.; Belletete, M.; Durocher, G.; Tao, Y.; Leclerc, M. Toward a Rational Design of Poly(2,7-Carbazole) Derivatives for Solar Cells. *J. Am. Chem. Soc.* **2008**, *130*, 732−742.

(4) Chen, M. H.; Hou, J.; Hong, Z.; Yang, G.; Sista, S.; Chen, L. M.; Yang, Yang. Efficient Polymer Solar Cells with Thin Active Layers Based on Alternating Polyfluorene Copolymer/Fullerene Bulk Heterojunctions. *Adv. Mater.* **2009**, *21*, 4238−4242.

(5) (a) Chen, H. Y.; Hou, J.; Zhang, S.; Liang, Y.; Yang, G.; Yang, Y.; Yu, L.; Wu, Y.; Li, G. Polymer Solar Cells with Enhanced Open-Circuit Voltage and Efficiency. *Nat. Photonics* **2009**, *3*, 649−653. (b) Hou, J.; Chen, H. Y.; Zhang, S.; Chen, R. I.; Yang, Y.; Wu, Y.; Li, G. Synthesis of a Low Band Gap Polymer and Its Application in Highly Efficient Polymer Solar Cells. *J. Am. Chem. Soc.* **2009**, *131*, 15586−15587.

(6) Huo, L.; Hou, J.; Zhang, S.; Chen, H. Y.; Yang, Y. A Polybenzo[1,2-*b*:4,5-*b*′]dithiophene Derivative with Deep HOMO Level and Its Application in High-Performance Polymer Solar Cells. *Angew. Chem., Int. Ed.* **2010**, *49*, 1500−1503.

(7) (a) Zhang, G.; Fu, Y.; Zhang, Q.; Xie, Z. Benzo[1,2-b:4,5-b′]dithiophene-dioxopyrrolothiophen Copolymers for High Performance Solar Cells. *Chem. Commun.* **2010**, *46*, 4997−4999. (b) Zou, Y.; Najari, A.; Berrouard, P.; Beaupre, S.; Aïch, B. R.; Tao, Y.; Leclerc, M. A Thieno[3,4-*c*]pyrrole-4,6-dione-Based Copolymer for Efficient Solar Cells. *J. Am. Chem. Soc.* **2010**, *132*, 5330−5331.

(8) (a) Price, S. C.; Stuart, A. C.; Yang, L.; Zhou, H.; You, W. Fluorine Substituted Conjugated Polymer of Medium Band Gap Yields 7% Efficiency in Polymer−Fullerene Solar Cells. *J. Am. Chem. Soc.* **2011**, *133*, 4625−4631. (b) Huang, Y.; Huo, L.; Zhang, S.; Guo, X.; Han, C. C.; Li, Y.; Hou, J. Sulfonyl: A New Application of Electron-Withdrawing Substituent in Highly Efficient Photovoltaic Polymer. *Chem. Commun.* **2011**, *47*, 8904−8906.

(9) Li, Y. Molecular Design of Photovoltaic Materials for Polymer Solar Cells: Toward Suitable Electronic Energy Levels and Broad Absorption. *Acc. Chem. Res.* **2012**, *45*, 723−733.

(10) Huang, Y.; Guo, X.; Liu, F.; Huo, L.; Chen, Y.; Russell, T. P.; Han, C. C.; Li, Y.; Hou, J. Improving the Ordering and Photovoltaic Properties by Extending π−Conjugated Area of Electron-Donating Units in Polymers with D-A Structure. *Adv. Mater.* **2012**, *24*, 3383−3389.

(11) Hou, J.; Tan, Z.; Yan, Y.; He, Y.; Yang, C.; Li, Y. Synthesis and Photovoltaic Properties of Two-Dimensional Conjugated Polythiophenes with Bi(thienylenevinylene) Side Chains. *J. Am. Chem. Soc.* **2006**, *128*, 4911−4916.

(12) Hou, J.; Tan, Z.; He, Y.; Yang, C.; Li, Y. Branched Poly(thienylene vinylene)s with Absorption Spectra Covering the Whole Visible Region. *Macromolecules* **2006**, *39*, 4657−4662.
(13) Klauk, H.; Halik, M.; Zschieschang, U.; Schmid, G.; Radlik, W.; Weber, W. High-Mobility Polymer Gate Dielectric Pentacene Thin Film Transistors. *J. Appl. Phys.* **2002**, *92*, 5259−5263.
(14) Huo, L.; Zhang, S.; Guo, X.; Xu, F.; Li, Y.; Hou, J. Replacing Alkoxy Groups with Alkylthienyl Groups: A Feasible Approach to Improve the Properties of Photovoltaic Polymers. *Angew. Chem., Int. Ed.* **2011**, *123*, 9871−9876.
(15) (a) Huo, L.; Ye, L.; Wu, Y.; Li, Z.; Guo, X.; Zhang, M.; Zhang, S.; Hou, J. Conjugated and Nonconjugated Substitution Effect on Photovoltaic Properties of Benzodifuran-Based Photovoltaic Polymers. *Macromolecules* **2012**, *45*, 6923−6929. (b) Duan, R.; Ye, L.; Guo, X.; Huang, Y.; Wang, P.; Zhang, S.; Zhang, J.; Huo, L.; Hou, J. Application of Two-Dimensional Conjugated Benzo[1,2-*b*:4,5-*b*′]dithiophene in Quinoxaline-Based Photovoltaic Polymers. *Macromolecules* **2012**, *45*, 3032−3038.
(16) (a) Wienk, M. M.; Turbiez, M.; Gilot, J.; Janssen, R. A. J. Narrow-Bandgap Diketo-Pyrrolo-Pyrrole Polymer Solar Cells: The Effect of Processing on the Performance. *Adv. Mater.* **2008**, *20*, 2556−2560. (b) Huo, L.; Hou, J.; Chen, H. Y.; Zhang, S.; Jiang, Y.; Chen, T. L.; Yang, Y. Bandgap and Molecular Level Control of the Low-Bandgap Polymers Based on 3,6-Dithiophen-2-yl-2,5-dihydropyrrolo-[3,4-*c*]pyrrole-1,4-dione toward Highly Efficient Polymer Solar Cells. *Macromolecules* **2009**, *42*, 6564−6571. (c) Kanimozhi, C.; Balraju, P.; Sharma, G. D.; Patil, S. Synthesis of Diketopyrrolopyrrole Containing Copolymers: A Study of Their Optical and Photovoltaic Properties. *J. Phys. Chem. B.* **2010**, *114*, 3095−3103.
(17) (a) Ha, J. S.; Kim, K. H.; Choi, D. H. 2,5-Bis(2-octyldodecyl)-pyrrolo[3,4-*c*]pyrrole-1,4-(2*H*,5*H*)-dione-Based Donor−Acceptor Alternating Copolymer Bearing 5,5′-Di(thiophen-2-yl)-2,2′-biselenophene Exhibiting 1.5 $cm^2 \cdot V^{-1} \cdot s^{-1}$ Hole Mobility in Thin-Film Transistors. *J. Am. Chem. Soc.* **2011**, *133*, 10364−10367. (b) Tandy, K.; Dutta, G.; Zhang, Y.; Venkatramaiah, N.; Aljada, M.; Burn, P. L.; Meredith, P.; Namdas, E. B.; Patil, S. A New Diketopyrrolopyrrole-Based Co-Polymer for Ambipolar Field-Effect Transistors and Solar Cells. *Org. Electron.* **2012**, *13*, 1981−1988.
(18) Bijleveld, J. C.; Zoombelt, A. P.; Mathijssen, S. G. J.; Wienk, M. M.; Turbiez, M.; de Leeuw, D. M.; Janssen, R. A. J. Poly-(diketopyrrolopyrrole −terthiophene) for Ambipolar Logic and Photovoltaics. *J. Am. Chem. Soc.* **2009**, *131*, 16616−16617.
(19) Ye, L.; Zhang, S.; Ma, W.; Fan, B.; Guo, X.; Huang, Y.; Ade, H.; Hou, J. From Binary to Ternary Solvent: Morphology Fine-tuning of D/A Blends in PDPP3T-based Polymer Solar Cells. *Adv. Mater.* **2012**, *24*, 6335−6341.
(20) Dou, L.; You, J.; Yang, J.; Chen, C. C.; He, Y.; Murase, S.; Moriarty, T.; Emery, K.; Li, G.; Yang, Y. Tandem Polymer Solar Cells Featuring a Spectrally Matched Low-Bandgap Polymer. *Nat. Photonics* **2012**, *6*, 180−185.
(21) Bronstein, H.; Chen, Z.; Ashraf, R. S.; Zhang, W.; Du, J.; Durrant, J. R.; Tuladhar, P. S.; Song, K.; Watkins, S. E.; Geerts, Y.; et al. Thieno[3,2-b]thiophene-Diketopyrrolopyrrole-Containing Polymers for High-Performance Organic Field-Effect Transistors and Organic Photovoltaic Devices. *J. Am. Chem. Soc.* **2011**, *133*, 3272−3275.
(22) Sonar, P.; Singh, S. P.; Li, Y.; Soh, M. S.; Dodabalapur, A. A Low-Bandgap Diketopyrrolopyrrole-Benzothiadiazole-Based Copolymer for High-Mobility Ambipolar Organic Thin-Film Transistors. *Adv. Mater.* **2010**, *22*, 5409−5413.
(23) Li, Y.; Cao, Y.; Gao, J.; Wang, D.; Yu, G.; Heeger, A. J. Electrochemical Properties of Luminescent Polymers and Polymer Light-Emitting Electrochemical Cells. *Synth. Met.* **1999**, *99*, 243−248.
(24) Scharber, M. C.; Mühlbacher, D.; Koppe, M.; Denk, P.; Waldauf, C.; Heeger, A. J.; Brabec, C. J. Design Rules for Donors in Bulk-Heterojunction Solar Cells-Towards 10% Energy-Conversion Efficiency. *Adv. Mater.* **2006**, *18*, 789−794.
(25) Malliaras, G. G.; Salem, J. R.; Brock, P. J.; Scott, C. Electrical Characteristics and Efficiency of Single-Layer Organic Light-Emitting Diodes. *Phys. Rev. B* **1998**, *58*, 13411.
(26) Clarke, T. M.; Durrant, J. R. Charge Photogeneration in Organic Solar Cells. *Chem. Rev.* **2010**, *110*, 6736−6767.
(27) Guo, X.; Zhang, M.; Huo, L.; Xu, F.; Wu, Y.; Hou, J. Design, Synthesis and Photovoltaic Properties of a New D−π−A Polymer with Extended π-Bridge Units. *J. Mater. Chem.* **2012**, *22*, 21024−21031.